

# Plasma-Vehicle Interaction in a Plasma Stream

DAVID F. HALL,\* ROBERT F. KEMP,\* AND J. M. SELLEN JR.\*  
*TRW Space Technology Laboratories, Redondo Beach, Calif*

The electrical interaction, i.e., the sheath, of a spherical spacecraft traveling through the ionosphere is considered for two cases. For the case of vehicle velocity small compared to the thermal velocity of the ions, Poisson's equation is numerically integrated assuming a single initial ion velocity. Sample results of a simple computer program are presented. To study the case of vehicle velocity large compared to ion velocity, a "plasma wind tunnel" is used. Measurements in the plasma wind tunnel include plasma potentials near the sheath boundary, ion current density ( $j_+$ ) contours in the sphere's wake,  $j_+$  collected at various positions on the sphere surface, total ion current collected by the sphere, and the plasma's enhancement of the electric field at various positions on the sphere surface. Scaling relationships are discussed.

## Nomenclature

$v_s$	= velocity of sphere relative to a stationary earth, cm/sec
$v_+$	= average velocity of ions in the plasma relative to a stationary earth, cm/sec
$\rho_0$	= ambient plasma density, ions/cm <sup>3</sup>
$V_s$	= sphere potential relative to plasma potential, v
$r$	= radial distance from sphere's center, in
$k$	= Boltzmann's constant $1.38 \times 10^{-23}$ joules/°K
$T$	= Kelvin temperature
$i$	= current, amp
$U$	= velocity of ion beam, cm/sec
$E$	= electric field vector
$j_+$	= ion current density, amp/cm <sup>2</sup>
$\mathbf{r}$	= acceleration vector
$R_0$	= normalization unit of distance
$M_+$	= ion mass, amu
$m$	= electron mass, kg
$e$	= electron charge
$\sigma$	= net charge density, coul/m <sup>3</sup>
$\theta$	= angular coordinate of a point with respect to the origin at sphere center and the axis of sphere motion
$\epsilon_0$	= permittivity of free space, $8.8 \times 10^{-12}$ farads/m
$\gamma$	= electric field strength enhancement at vehicle surface

## Subscripts

+	= ion
—	= electron
s	= sphere
b	= button
pb	= boundary of the undisturbed plasma
0	= initial or ambient
f	= final
tot	= total

## Introduction

THE following paper examines the electrical interaction between a spherical spacecraft and its environment. This environment consists of a dilute collisionless plasma whose density  $\rho_0$  ranges from a maximum of about  $10^6$  ions/cm<sup>3</sup> at an altitude of several hundred kilometers to about  $10^3$  ions/cm<sup>3</sup> at several thousand kilometers.

The potential  $V$  relative to the ambient plasma potential that a vehicle acquires from the kinetic energies of particles in the plasma will be only a few volts different from the plasma potential.<sup>1</sup> However, if the vehicle carries an electric

propulsion device, a small unbalance in the number of negative- and positive-charge carriers expelled can result in a  $V_s$  of many volts. This, in turn, can lead to large electrical interactions, as will be shown. In all subsequent discussions,  $V_s$  is regarded as an independent variable. However, the situation is idealized by omitting consideration of a plasma thrust beam in any local effects that it might have on fields and potentials in the sheath.

Two cases are considered. The first is for  $v \ll v_+$ , where  $v$  is the sphere velocity and  $v_+$  the average thermal velocity of the ions in the plasma, both relative to a stationary earth. In this "stationary vehicle" case a simple numerical treatment yields useful estimates of the electrical interaction. The second, and more interesting case is when  $v \gg v_+$ . This condition obtains for a vehicle orbiting the earth in the ionosphere and for large portions of probe shots. The relative velocity  $U$  between the vehicle and the ions in the plasma destroys the spherical symmetry important to a simple mathematical treatment.

This more involved "moving vehicle" case has been treated numerically by Davis and Harris.<sup>2</sup> In the work described in this paper, an experimental approach, using a "plasma wind tunnel," has been employed. The areas of agreement between the behavior calculated in Ref. 2 and these experimental studies are discussed. In general, experimental parameters are as follows:  $3 \times 10^5 \leq \rho_0 \leq 1.2 \times 10^7$  ions/cm<sup>3</sup>,  $-400 \leq V \leq 0$  v,  $r = 0.37$  or  $1$  in,  $U = 7.7$  or  $11$  km/sec. The sphere radius is  $r$ .

These ranges of the parameters do not represent constraints imposed by the experimental techniques. The methods to be described can be employed to study a broad variety of plasma-vehicle systems. The section that discusses scaling parameter values broadens their applicability even further.

The electrical interaction between a plasma and a conductor manifests itself as a region of disturbed plasma called the sheath. This sheath represents equilibrium values for the electric field strength  $E$  and the currents of charge carriers at every point "near" the conductor. The basic quantities of interest are  $E(r, \theta)$ , particularly at  $r$  and  $r_{pb}(\theta)$ , where  $r$  and  $\theta$  are, respectively, the radial and angular coordinates of a point, with respect to the origin of coordinates at the center of the sphere and a line,  $\theta = 0$ , in the direction of the sphere's motion through the plasma. The subscript  $pb$  refers to the sheath-plasma boundary. Another area in which attention may be usefully directed in the case of the moving vehicle, is the description of the ion trajectories through the sheath.

In addition to being interesting in its own right, the information just outlined contributes to the solution of several practical problems. Electric propulsion specialists would

Presented as Preprint 63055 at the AIAA Electric Propulsion Conference, Colorado Springs, Colo., March 11-13, 1963; revision received March 18, 1964. This work supported by NASA Lewis Research Center (Contract NAS8-1560).

\* Member of the Technical Staff. Member AIAA.

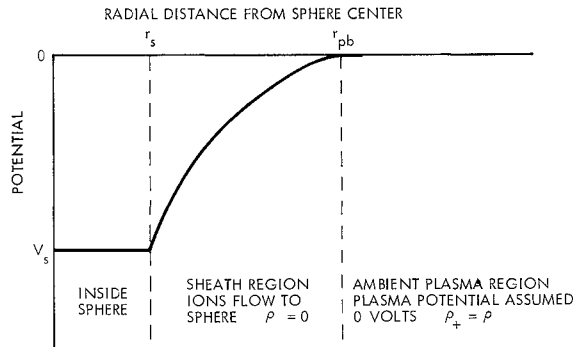


**Fig 1 Potential diagram of a stationary sphere immersed in a plasma**

like a means for monitoring the potential of a vehicle, since it is a strong function of beam neutralization. This may be achieved with a knowledge of  $E_s$  at the vehicle surface and of the shape of the field within the sheath. Instruments are available for measuring the former, but without the latter,  $V_s$  is known only very approximately. Without knowledge of the  $\theta$  dependence of  $\mathbf{E}$ , signals from a tumbling vehicle would be particularly difficult to interpret.

Another reason for studying details of the sheath is their importance to the electrical drag on a vehicle. Drag results from a momentum interchange between the vehicle and the apparently ordered plasma flow.

Finally, this sort of information may lead to new techniques for using satellites to examine the ionospheric plasma.

The first section is a brief mathematical treatment of the stationary case. The second describes measurements made in a plasma wind tunnel. They include studies of plasma potentials near the sheath boundary, ion current density ( $j_+$ ) contours in the sphere's wake,  $j_+$  collected at various positions on the sphere surface, total ion current collected by the sphere, and the plasma's enhancement of the electric field at various positions on the sphere surface. The third section discusses scaling relationships.

### Mathematical Treatment of Stationary Case

For that condition in which  $v \ll v_+$ , the plasma-vehicle interaction may be calculated. The problem is essentially that of a spherical electrostatic probe in a plasma, which has been treated in varying degrees of completeness by Langmuir<sup>3,4</sup> and co-workers, Allen, et al.,<sup>5</sup> Medicus,<sup>6</sup> Bernstein and Rabinowitz,<sup>7</sup> and by others. Since neither the ionic constituents nor the ion and electron kinetic energy distributions of the ionosphere are known with precision, an involved theoretical treatment is not warranted. However, useful estimates of sheath size can be provided for the condition  $|V_s| \gg kT_+/e$  (a condition of considerable interest when vehicles bear electrical propulsion devices) by the following simple numerical technique.

The existence of a vehicle with  $V_s < 0$  in a plasma of potential  $V = 0$  results in the potential diagram of Fig 1. In reality, ions that diffuse to a given point on the sheath boundary will have a distribution in both velocity and direction. It is assumed here that, while undergoing diffusion, the ions may be represented as having a single average velocity  $v_+$ . When they reach the sheath edge, the additional assumption is made that all velocities are radial. Another simplification employed in the calculation is that electrons diffusing toward the sphere are repelled at the surface  $r = r_{pb}$ , which leads to the boundary condition  $dV/dr = 0$  at  $r = r_{pb}$ . In reality, the electrons are deflected over a region of finite thickness, and  $dV/dr$  may have a small positive value at the surface designated  $r_{pb}$ . A final assumption, probably quite accurate, is thermal equilibrium in the plasma:  $M_+v_+^2 = mv_-^2$ .

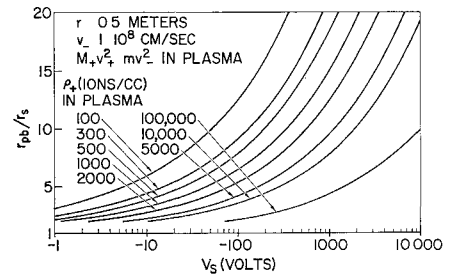


**Fig 2 The ratio of sheath radius to sphere radius as a function of sphere potential for various particle densities in a plasma**

The current density that diffuses to the sheath boundary is  $j_{0+} = \rho_0 v_+/4$ . From the conservation of charge, in the sheath,  $j_+ = j_{0+} r_{pb}^2 / r^2$ . From the conservation of energy, the ion velocity in the sheath is given by  $[(2e/M_+)(V + V_0)]^{1/2}$  where  $V_0 = M_+ v_+^2 / 2e$ . Therefore, Poisson's equation becomes

$$\frac{d^2 V}{dr^2} + \frac{2}{r} \frac{dV}{dr} = - \frac{r_{pb}^2 \rho_0 v_+}{4\epsilon_0 r^2 [(2e/M_+)(V + V_0)]^{1/2}} \quad (1)$$

The equation is solved by setting the parameters  $r_s$ ,  $\rho_0$ , and  $v_+$ , choosing a value of  $r_{pb}$ , and then numerically integrating Eq (1) from  $r_{pb}$  to  $r_s$  on a computer. Values of  $V(r)$  and  $dV(r)/dr$  are printed.

An example of the results obtained is given in Fig 2. It displays  $r_{pb}/r_s$  as a function of  $V_s \equiv V(r)$  for several  $\rho_0$ . The densities have ranged from 100–100,000 ions/cm<sup>3</sup> which approximately corresponds to densities encountered from the protonosphere downward to an altitude of about 500 km. The vehicle radius has been held fixed at 0.50 m.

The results given in Fig 2 are shown with  $V_s < 0$ . They are equally valid, however, for  $V_s > 0$  under the assumption of a thermal equilibrium in the plasma. In fact, for a given plasma temperature, the shape of  $|V(r)|$  is independent of particle mass and sign, although the current to the sphere is not.

From the results of these calculations, it may be noted that the extent of the sheath may be many times greater than the physical size of the vehicle. The size of the sheath is increased for increased  $V_s$  and is diminished by an increase in  $j_0$  in the plasma through an increase in the number density. If  $j_0$  is increased by increasing the particle energy, the sheath size is also diminished.<sup>8</sup>

The dependability of these results may be discussed in terms of the simplifying assumptions mentioned earlier. The assumption  $V_s \gg kT_+/e$  assured that 1) the distribution of initial velocities could be accurately represented by a single value  $v_+$ , and 2) ions with initial velocities other than radial would still be collected. For  $|V_s| < 10$  v and  $\rho_0 < 10^3$  ions/cm<sup>3</sup>, this condition begins to fail, and some

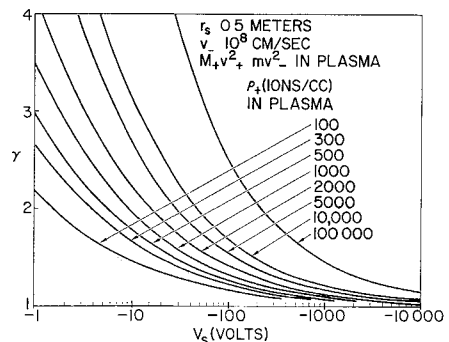


**Fig 3 Electric field enhancement at sphere's surface as a function of sphere potential for various particle densities in a plasma**

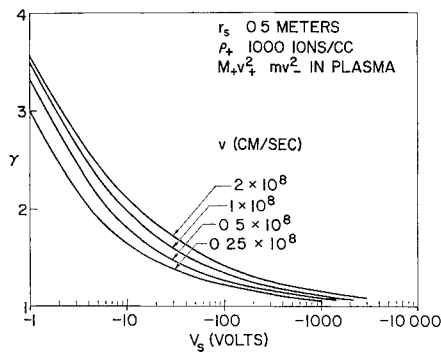


Fig 4 Electric field enhancement at sphere's surface as a function of sphere potential for various electron energies

ions are scattered rather than collected. However, if *all* ions were scattered, this would only double the effective value of  $\rho$  (since each ion would then contribute to the space charge as it moved away from the sphere as well as while approaching it). Thus, results presented in Fig 2 may be about a factor of 2 low in ion density for the low-density, low-sphere-potential region.

A second aspect of the interaction between the vehicle and the plasma is the enhancement of  $E$  at the vehicle surface. Lines of force from surface charges on the vehicle no longer terminate at infinity, as they do in a perfect vacuum, but, instead, terminate within the sheath. This creates a greater initial  $dV/dr$  for a given  $V_s$  than exists in the vacuum case. The enhancement of  $E$  at the surface is expressed by  $\gamma$ :

$$E_s|_{\text{plasm}} = \gamma E_s|_{\text{vacuum}} \quad (2)$$

Figures 3 and 4 present the results of numerical evaluation of  $\gamma$  as a function of  $V_s$  for a series of  $\rho_0$  and  $v_-$ . Field strength enhancement increases with  $\rho_0$  and with  $v_-$ , indeed, with any variation of conditions which diminishes the extent of the sheath.

It is of interest to know at what time during a vehicle's trajectory the foregoing results will apply, i.e., when is  $v \ll v_+$ ? This question is involved because different ionic species exist at different altitudes. Their mass, the sunspot cycle, and the time of day all affect  $v_+$ . As a rough indication, a vehicle undergoing free fall from an initial altitude of 4000 miles would begin to experience  $v \geq v_+$  at  $\approx 1700$  miles.<sup>9</sup> For a vehicle orbiting below the protonosphere,  $v$  will always exceed  $v_+$ .

When  $v > v_+$ , the particles in the plasma no longer possess, in the reference frame of the vehicle, the purely random thermal motion assumed in the forementioned calculation. Instead, the positive charge carriers possess an ordered

streaming velocity  $U$ . Spherical symmetry no longer obtains as the region in front of the advancing vehicle differs from that region to the rear of the vehicle. Under these circumstances, a calculation of the vehicle-plasma interaction becomes extremely complicated. Some aspects of the problem have been treated numerically by Davis and Harris.<sup>2</sup> The following work experimentally duplicates that condition in which a relative motion exists between the vehicle and the plasma by directing a plasma stream against a stationary vehicle.

## Experimental Measurements

### The Experimental Array

The situation of a vehicle traveling through a plasma at considerable speed is simulated in the laboratory with the array indicated in Fig 5. An ion beam from a 1-in.-diam porous tungsten source is neutralized by injection of electrons, and the resultant plasma beam is directed against a model vehicle. Ions are accelerated by the potential difference between the source and a planar grid, separated from the tungsten source by a distance which is an order of magnitude smaller than the beam diameter. The beam currents are space charge limited, typical operating conditions giving beam current of 3 ma at a net accelerating potential of 90 v. Because of the large aspect ratio of the emitter-grid assembly, the ion beam would have demonstrated violent space charge perturbations, including reversal of ion motion, had adequate neutralization not been provided through injection of electrons.<sup>10</sup> The electron source used for most of the measurements is a tungsten wire located about one-half inch from the beam axis. A potential of a few volts is developed between this cathode and the beam. This results in injecting electrons at a relatively high energy, and a broad, dilute beam is produced by the pressure of these electrons on the radial boundaries of the beam. Another electron source, fully immersed in the beam, also could be used. It yielded the required neutralization current with electron velocities corresponding to a fraction of a volt and produced smaller beam divergence. Thus, electron temperature in the beam varies inversely with  $\rho_0$  between a fraction of a volt to several volts.

Figure 5 also indicates the principal instruments used in this laboratory for plasma diagnosis. The emissive probe measures plasma potential. Its theory is discussed below. A Faraday cup probe (hereafter abbreviated  $j_+$  probe), for measuring ion current density, is shown. The entire end of the vacuum chamber is covered with a segmented collector, which provides a quick measure of the radial extent and uniformity of the beam. The emissive and  $j_+$  probes may be moved within the beam as indicated.

The accelerating voltage for the beam is a periodic pulse train of rectangular waveform, making possible the continuous read-out of diagnostic information concerning the beam. Included are such items as ion transit time and the initial shape of  $j_+$  and beam current signals.

Background pressures in the vacuum systems ranged from 1 to  $2 \times 10^{-6}$  torr, corresponding to neutral densities of 3 to  $6 \times 10^{10}$  particles/cm<sup>3</sup>, and a mean free path of the order of  $10^3$  m.

In the emissive probe measurements to be described, the distance between the plasma source and the sphere is 80 cm, and the distance between the sphere and the (electrically) floating collector at the end of the chamber is about 10 cm. In all other measurements, the plasma source to sphere distance is 2 m, and the sphere to collector distance about 25 cm. Thus, in the region of the sphere, the incident ions are quite paraxial.

The velocity of the ions  $U$  was determined both by measuring the time of flight of a small marker pulse put on the beam and by measuring the applied acceleration voltage. Either technique easily provides the velocity within 2%.

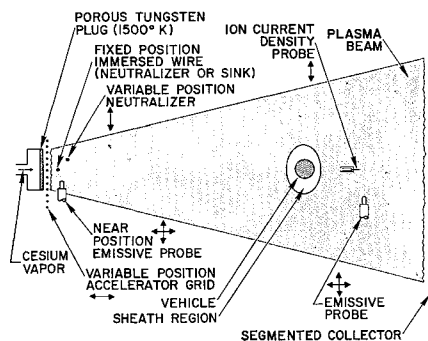


Fig 5 Experimental array. The plasma beam is directed against the model vehicle. Plasma diagnosis is performed using emissive probes, Langmuir probes,  $j_+$  probes, and the segmented collector. Neutralization of the ion beam is achieved through either fixed or variable-position hot-wire neutralizers.

A 68 cm<sup>2</sup> Faraday cup located on the beam axis provided the value of  $\rho_0$  through  $\rho_0 = j_+/U$ . This cup was fitted with grid wires across its opening which could be biased to retain secondary electrons. Its current was measured with an oscilloscope to  $\sim 3\%$ .

In the experiments to be described, ions are collected by the sphere. It is considered that these ions are neutralized upon contact with the sphere surface and are subsequently removed, for the most part, by a combination of sputtering and evaporation.

### Emissive Probe

An emissive probe measures local plasma potentials. It may be constructed by spot welding a "hairpin" filament of 0.001-in.-diam tungsten wire  $\frac{1}{4}$  in. long to conductors placed in a two-hole ceramic rod. The rod, in turn, is slipped through thin-walled stainless-steel tubing, which provides support and shielding of the probe supports from ion bombardment. Electrically, the tubing is allowed to float in order to minimize its perturbation of the plasma.

This filament is made emissive by heating it to a thermionic temperature. So that it will be unipotential during the measurement, it is customarily heated with half-wave-rectified a c synchronized with the pulsing of the beam. Its potential, with respect to the plasma, is controlled by a variable d c supply.

The theory of the emissive probe is that, when the probe potential is below the plasma potential, probe current is emission limited. As the probe potential passes through the plasma potential, it begins to see a retarding potential that exponentially reduces the emission current. Therefore, a semilog plot of emission current vs probe voltage will have a shape as indicated in Fig. 6, the cutoff slope corresponding to filament temperature. The sharpness of the break between the horizontal emission-limited part of the curve and the diagonal retarding-potential section (the Boltzmann line) depends on factors such as the plasma density and the probe temperature. It is usually possible to produce a curve in which asymptotes to the two sections may be uniquely drawn. The intersection of these asymptotes is taken as the plasma potential.

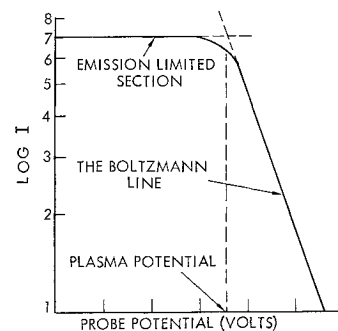
There are currents other than the emission current, which should be discussed. The probe collects ion current in proportion to the part of its surface area "seen" by the unidirectional ions. Since this area is very small, the ion current is negligible. When the probe is above the plasma potential, it will collect electrons from the plasma. This electron current is a function of the potential difference between the probe and the plasma potential. Since a current measuring device in the probe circuit can measure only the *net* electron flow from (or to) the filament, some provision must be made to insure that the current collected from the plasma does not grossly affect the slope and shape of the Boltzmann line. This may be accomplished by momentarily dropping the temperature of the filament until it is no longer emissive but is still warm and, therefore, of constant work function. The difference between the current measurements at these two temperatures is the emission current.

In summary, an emissive probe is a device capable of measuring local plasma potentials with an accuracy of from 0.01–0.1 v, depending on the plasma density, plasma turbulence, and the care employed in the measurement.

### Plasma Potentials near the Sheath Boundary

It was mentioned in the Introduction that, in the moving vehicle case, the shape of the boundary of the sheath around the vehicle and the potential contours along various radii are unknown and of interest. The emissive probe, with its ability to measure local potentials, is an excellent instrument for measuring these quantities. It is suspected, however, that when the probe protrudes very far into the sheath,

Fig. 6 Typical characteristic of an emissive probe



its physical size and its emission may seriously perturb the sheath. It has been observed that in these locations the knee of the probe characteristic becomes less sharp, and the slope of the Boltzmann line becomes higher in temperature than in the undisturbed plasma. Therefore, attention is restricted to the shape of the sheath boundary and the *initial* curvature of the potential contour.

An electronic system was devised which automated the data taking.<sup>8</sup> It enabled a complete set of data to be taken in a single operational period, which insured that the beam characteristics remained constant throughout the measurement.

Measurements were taken after the beam had reached the collector and, thus, had achieved an equilibrium condition. The collector was allowed to "float," so that it removed equal currents of ions and electrons from the beam.

It was found convenient to employ probe position as a parameter and sphere potential as the independent variable. Cross plots of the resulting data, taken along the three principal radii of the sphere (viz., the upstream direction, the sideward direction, and the downstream direction) were made to derive the potential contours shown in Figs. 7, 8, and 9, respectively. Sphere potential is measured relative to the plasma potential. They give a general idea of the potential contours of the sheath at and near its interface with the unperturbed resident plasma. In fact, from a partial contour, something may be deduced about its shape further into the sheath, since its end points, the plasma potential, and the surface potential of the sphere, are known. For instance, if, for a given sheath thickness, the curvature of the potential contour is initially small, then it is clear that closer to the negative sphere it must be large.

Upstream of the sphere, with  $V_s = -4.7$ ,  $\rho$  is expected to be substantial. If present in sufficient number, ions close to the sphere are able to terminate all the electric field lines leaving the sphere in the upstream direction. This may be thought of as a "screening" effect. Since the  $V_s = -4.7$  curve in Fig. 7 has a small initial curvature, we may

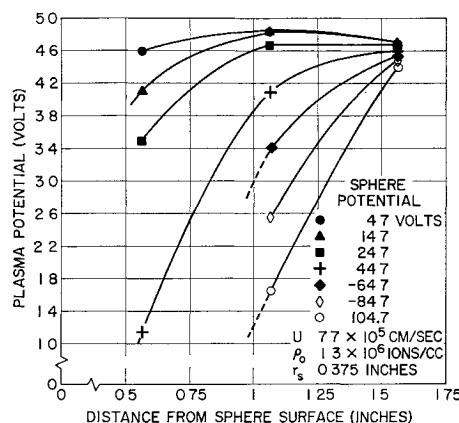


Fig. 7 Potential contours of the sphere's sheath in the upstream direction for various sphere potentials. Ions in the beam are 41 ev.

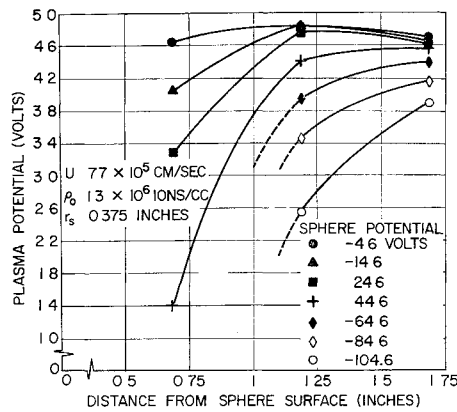


Fig 8 Potential contours of the sphere's sheath in the sideward direction for various sphere potentials Ions in the beam are 41 ev

infer that screening does take place, and that the curvature is increased in the region of enhanced charge density

At large negative values of sphere potential, one might expect this screening effect to diminish in the upstream direction because  $\rho$  diminishes (owing to increased  $v_+$ ). In fact, it takes only  $-75$  v on the sphere to make the sheath extend  $1\frac{1}{8}$  in from the surface, compared to  $-130$  v required in the rear for a similar effect. It will be shown later that  $\rho$  is rather large to the rear under such conditions

At the side of the sphere, with low negative  $V_s$ , the initial curvature of the potential contour suggests that  $\rho$  is a little smaller than in the front. However, at large negative voltages,  $\rho$  at the side must be considerably smaller than in either the front or the rear. Only  $-50$  v is required to extend the sheath  $1\frac{1}{8}$  in in this direction

Downstream of the sphere, with  $V_s = 0$ , one would expect a cylindrical volume substantially devoid of ions. Measurements with a  $j_+$  probe, to be described later, confirm this expectation. With an absence of positive ions in this region to terminate field lines leaving the sphere, the potential contours should be close to the vacuum  $1/r$  relationship. Hence, the sheath is relatively large as is the initial curvature of the potential contour. This is seen in Fig 9

At small values of  $V_s$  (both negative and positive), an interesting effect is seen in the downstream region. When the emissive probe is positioned at either 1 or  $1\frac{1}{2}$  in, a negative value of  $V_s$  raises the plasma potential, and conversely. Undoubtedly, these are ion and electron optical effects. It is this initial increase in potential with negative sphere voltage which relates to the crossing of the potential

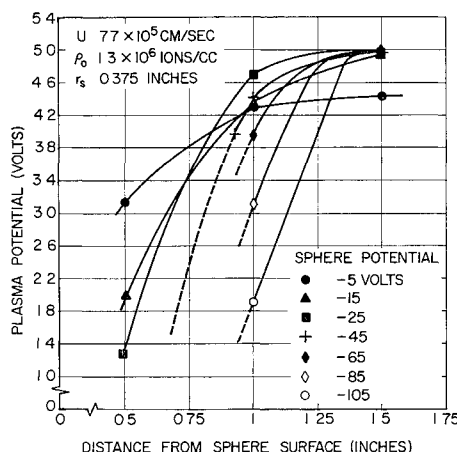


Fig 9 Potential contours of the sphere's sheath in the downstream direction for various sphere potentials Ions in the beam are 41 ev

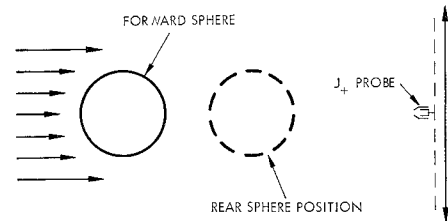


Fig 10 Schematic of measurements of ion current density in the wake

contours in Fig 9. Deflection of large numbers of ions behind the sphere must occur at moderate and large negative potentials;  $-130$  v is required to extend the sheath to  $1\frac{1}{2}$  in. Other evidence of such gross deflection will be presented later

The foregoing data provide a rather unexpected picture of the shape of the sheath. At low negative sphere potentials, it is short and steep in front, relatively long and gradual at the rear. At negative potentials in excess of  $-50$  v the sheath is shortest in the rear and thickest at the sides; something like the sheath depicted in Fig 5

### Ion Current Density in the Wake

Another approach to the study of the plasma-vehicle interaction is to observe the deflection of (initially paraxial) ions by electric fields associated with the vehicle. This section deals with those ion trajectories that are made to pass through the downstream "shadow" region of the vehicle. The next section treats those trajectories that impact the sphere

The scheme for observing  $\rho$  in the wake is shown in Fig 10. Either of two spheres could be positioned on the beam axis. When one was used, the other was withdrawn from the beam. Thus, two sphere-to-probe distances were provided. The  $j_+$  probe was moved along a path perpendicular to the beam axis, 7 in downstream of the forward sphere center, and 4 in downstream of the center of the other sphere

Figure 11 shows data collected in this manner. The "0" on the abscissa corresponds to locating the probe directly behind the sphere. Notice that when the sphere is at its floating potential, the current density behind the sphere is very small. This region has about the same diameter as the

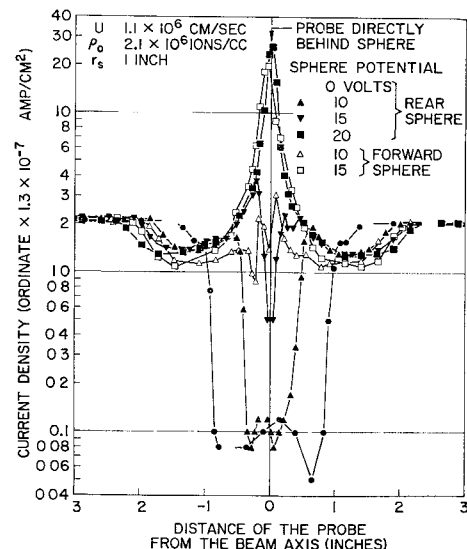


Fig 11 Ion current density contours of the sphere's wake for several potentials. Curves of "rear" sphere were taken 4 in downstream of sphere center; the "forward" sphere curves were taken 7 in downstream. Ions in the beam are 90 ev

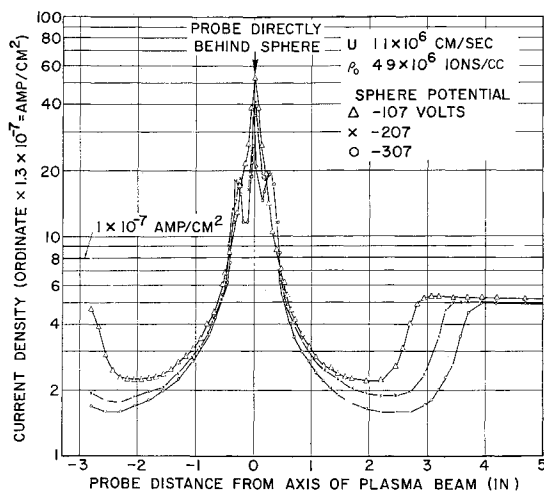


Fig 12 Ion current density contours of the rear sphere's wake for several sphere potentials (taken 4 in downstream of sphere center) Ions in the beam are 90 ev

sphere itself, 2 in. A similar curve for the forward sphere had a "shadow"  $\frac{1}{16}$  in less in width.

When the sphere was made negative, there was clear evidence that ions traveling at considerable distances from the beam axis were deflected. This caused the symmetrically scooped regions in the current density contour on either side of the sphere. Some of these ions were collected by the sphere; others were deflected into the region behind it, causing the large peaks shown there. It was found that the more negative the sphere and the more dilute the plasma, the greater the diameter of the zone of disturbance to the side of the sphere.

Figure 11 shows the sensitive response of  $j_+$  behind the sphere to the application of small negative  $V_s$ . At a given distance from the sphere, the shadow diameter decreases to zero, then a sharp peak in  $j_+$  appears on the axis. This peak forms at 7 in downstream with 90-ev ions, for a  $V_s$  of only -15 v. An additional -5 v cause the peak to appear 3 in closer. Figure 12, however, demonstrates that, in the range of  $V_s$  between -300 v and -100 v, no further change in the peak was noted. The data in Fig 13, taken at smaller  $\rho_0$ , confirm this result, and show that for large negative  $V_s$ , the  $j_+$  contours are nearly the same at different distances from the sphere. From these results, one is led to visualize the formation of a high-density "tail" that trails along the line of vehicle motion in the downstream direction. This high-density core results from the compression of ion trajectories drawn from a finite-area annulus surrounding the sphere into the zero area (in principle) of the axis. The peaks to the side of the central peak are caused by the combination of ions that have crossed over the beam axis with some of those which have yet to cross it. Since  $\rho_+ = \rho_-$  in this tail, it is not proper to regard it as part of the sheath.

These wakes, with their low-density regions to the side and their high-density axial cores, have all the essential features of those calculated by Davis and Harris<sup>2</sup>. They have "a low density region occupying most of the space behind the object and extending to a somewhat larger radius than the sphere itself" and "a small region, close to the axis, extending quite far behind the sphere where density reaches rather high values". They also are similar to those of a wire in a streaming mercury plasma observed by Meckel<sup>11</sup> under conditions of high mercury vapor pressure (0.001-5  $\mu$ ).

#### Ion Current Density on the Vehicle Surface

In order to measure the ion current density intercepted by various regions on the sphere surface, one point on the surface was fitted with a  $\frac{1}{8}$ -in-diam "button" sensor. Orien-

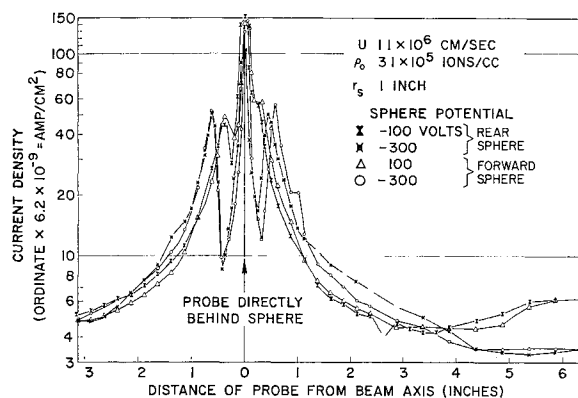


Fig 13 Ion current density contours of the sphere's wake for several sphere potentials Ions in the beam are 90 ev

tation of the button, whose current could be monitored, was provided by rotation of the entire sphere on its support rod, as indicated in Fig 14. Since the plasma-vehicle system possesses symmetry about the  $z$  axis, in principle, one needs only to vary  $\theta$  through  $180^\circ$  to map the current to every point on the sphere surface. When the button faces the plasma source,  $\theta$  is  $0^\circ$ .

Measurements made in this fashion are confused by the production of secondaries at button surfaces (including, perhaps, some interior to the sphere "seen" through the 10-mil gap between button and sphere). A more sophisticated sensor was devised to assess the effect of these secondaries. It consisted of a cross grid of six 1-mil wires across the aperture in the sphere and a Faraday cup behind the grid. This allowed the sensor to be biased without affecting fields outside the sphere.

The forementioned devices provide the following general picture of current density collected by the sphere: When  $V_s = 0$ , only the forward hemisphere collects current. A similar behavior was previously demonstrated in the Explorer VIII satellite<sup>12</sup>. However, for a relatively dense beam ( $\rho_0 \approx 10^7$  ions/cm<sup>3</sup>), as  $V_s$  is made negative there is increasing current collection in the rear hemisphere, and eventually a maximum appears at  $\theta = 180^\circ$ . In the vicinity of  $V_s = -150$ , this maximum begins to exceed that of the forward hemisphere. As  $\rho_0$  is decreased, the size of the maximum at  $180^\circ$ , relative to the forward maximum, decreases. With  $V_s = -300$ , the  $180^\circ$  point becomes a minimum at  $\rho_0 \approx 3 \times 10^6$  ions/cm<sup>3</sup>.

Figure 15 indicates the trajectories suggested by these data. The peak in  $j_+$  at  $180^\circ$  is thought to result from the compression of trajectories from an initial annulus of large area down to the very small circular area of the button, as shown. The crossover of trajectories in the wake was suggested in

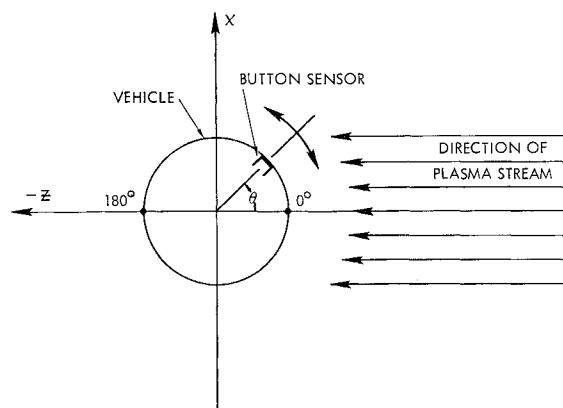


Fig 14 Schematic of measurement of ion current density to the sphere surface

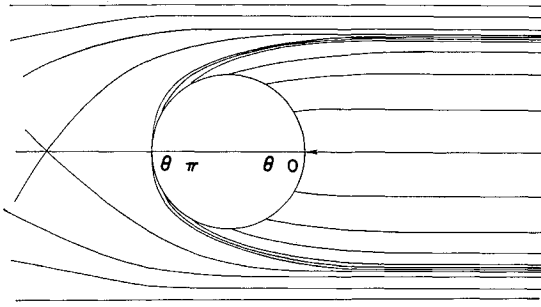


Fig 15 Approximate ion flow pattern Plasma incident from right is uniform in density

the last section. Attention is called to the similarity between these trajectories and those calculated by Davis and Harris.<sup>2</sup>

#### Total Ion Current to the Vehicle

The behavior of the total ion current  $i_{tot}$  as a function of  $V_s$  was found to be very nearly proportional to  $\rho_0$  for the entire range of  $V_s$ , when  $\rho_0$  was between  $1.5$  and  $3 \times 10^6$  ions/cm<sup>3</sup>. It is to be expected that  $i_{tot}$  would be proportional to  $\rho_0$  for small  $V_s$  in which there are substantially no deflections of ion trajectories and  $i_{tot}$  is given by  $\rho_0 v_+ \pi r^2$ . For large negative  $V_s$ , the sheath dimensions and ion trajectories do not remain independent of  $\rho_0$ . Since it was found that the proportionality between  $i_{tot}$  and  $\rho_0$  held even for  $V_s = -400$ , it is supposed that there are no substantial changes in the flow patterns when  $\rho_0$  is varied over the small range of  $1.5$ – $3 \times 10^6$  ions/cm<sup>3</sup>.

The total vehicle current also exhibits a behavior given approximately by

$$i_{tot} \approx i_{t0} \left( 1 + \frac{|V_s|}{V_0} \right) \quad (3)$$

where  $V_0$  is the ion acceleration voltage. Such behavior is to be expected in a system in which the electric fields are purely radial and there are no noncentral forces.<sup>6</sup> Although the plasma-vehicle interaction obviously is not a purely radial field configuration for these streaming plasmas, the occurrence of nonradial fields is not prominent enough to produce marked effects in the behavior of  $i_{tot}$ , and estimates of  $i_{tot}$  may be made from the simple relation just given.

#### Electric Field Strength on the Vehicle Surface

In the section, "Mathematical Treatment of Stationary Case," the electric field enhancement  $\gamma$  due to the near termination of lines of force in the sheath has been discussed, and calculations of  $\gamma$  are presented in Figs 3 and 4. It should be emphasized that these calculations are only valid

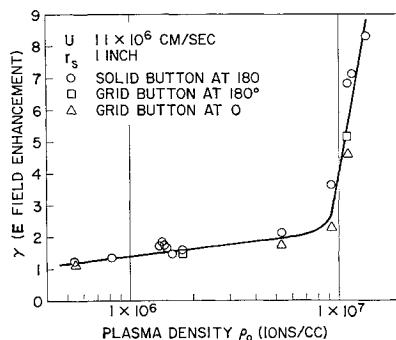


Fig 16 Electric field enhancement by sheath at 0° and 180° as a function of plasma density. Ions in the beam are 90 ev

for  $v \ll v_+$ . Using the sensor buttons in the vehicle and the techniques of a pulsed plasma beam, it is possible to measure  $\gamma$  for a streaming plasma.

Before the beam is pulsed on, the sphere is essentially isolated in a vacuum. Therefore,

$$E_0 = V_s/r \quad (4)$$

From Gauss' law, the total charge on the surface of the button, which forms a portion of the vehicle skin, is

$$Q_{b0} = \epsilon_0 E_0 A_b \quad (5)$$

After the beam has enveloped the sphere, the application of Gauss' law will give

$$Q_{b1} = \epsilon_0 E_1 A_b \quad (6)$$

From the foregoing, the new electric field strength may be expressed in terms of  $E_0$  and measurable  $\Delta Q$ :

$$E_1 = \frac{Q_{b1}}{\epsilon_0 A_b} = \frac{Q_{b0} + \Delta Q}{\epsilon_0 A_b} = E_0 + \frac{\Delta Q}{\epsilon_0 A_b} \quad (7)$$

This directly leads to a convenient expression for the electric field strength enhancement

$$\gamma = \frac{E_1}{E_0} = 1 + \frac{r_s}{\epsilon_0 A_b} \frac{\Delta Q}{V_s} \quad (8)$$

The experimentally determined charge  $\Delta Q$  flows during the time that the plasma stream engulfs the vehicle. This interval,  $\Delta t$ , is of the order of  $r_{pb}/v_+$ . By utilizing particular care in the formation of the pulsed beam, the leading edge of the plasma stream may be made comparatively "sharp" to assure a minimum elapsed time in the formation of the sheath. The minimization of this sheath formation time increases the magnitude of the observed current flow, since

$$i_b \approx \Delta Q / \Delta t \quad (9)$$

A further advantage of minimizing  $\Delta t$  is that often real ion currents are collected soon after the displacement currents occur, and if  $\Delta t$  is large, there is unnecessary overlap of these two signals.

Of course, to obtain  $\Delta Q$ , it is necessary to integrate  $i_b$  over the interval  $\Delta t$ . It was found convenient to record scope traces photographically, and later to perform the integration with a planimeter.

Somewhere in the range  $150^\circ \leq \theta \leq 90^\circ$ , collected ion currents begin to "obscure" the  $\Delta Q$  signal, depending on  $\rho_0$ . Therefore, a grid button was constructed by spot welding six 2-mil wires across the end of a  $\frac{1}{8}$ -in.-long piece of stainless thin-walled tubing. This resulted in a sensor whose physical projected area is  $\approx 0.2$  of its "effective electrical area" for  $\Delta Q$  signals.

The grid button was mounted diametrically opposite a solid button so that either could be oriented at any angle  $\theta$ .

The dependence of  $\gamma$  on  $\rho_0$  is given in Fig 16. Data collected with both the grid and the solid buttons are given. Each data point shown represents the value of the slope of lines from plots of  $\Delta Q$  vs  $V_s$  inserted into Eq (8). ( $\Delta Q$  vs  $V_s$  deviates from a linear relationship for high  $V_s$ .) Notice that, for a given value of  $\rho_0$ ,  $\gamma$  is always larger when  $\theta = 180^\circ$  than when  $\theta = 0^\circ$ . This is consistent with the sheath being shortest in the rear, as just reported.

It is not known why  $d\gamma/d\rho_0$  changes so radically at  $9 \times 10^6$  ions/cm<sup>3</sup>. Calculated values of  $\gamma$  for a stationary vehicle of this size, with  $V_s = -100$  and  $v_+ = 10^8$  cm/sec, range from  $1.7$ – $2.5$  over  $4 \times 10^6 \leq \rho_0 \leq 4 \times 10^7$  ions/cm<sup>3</sup>. This value of  $V_s$  was selected because, of the experimental values of  $V_s$  that were linear with  $\Delta Q$ , 100 v yields the greatest range in  $\gamma(\rho_0)$ .

#### Scaling Relationships

The question of scaling includes the physical scale of the model, the ion mass, and the ion velocity. One desires to

**Table 1** Three equivalent cases of a vehicle traveling through a plasma, showing the effect of changes in plasma density

	Case		
	I	II	III
$R_0$ , cm	5	5	5
$U$ , cm/sec	$1 \times 10^6$	$1 \times 10^6$	$1 \times 10^6$
$\rho_0$ , ions/cm <sup>3</sup>	$1 \times 10^7$	$1 \times 10^6$	$1 \times 10^5$
$M_+$ , amu	100	10	1
$V_s$ , v	-100	-10	-1

make measurements in a plasma wind tunnel in which ion trajectories have been scaled from the problem of interest. These trajectories are governed by

$$\frac{\ddot{\mathbf{r}}}{R_0} = \frac{e\mathbf{E}}{M_+R_0} \quad \text{and} \quad \mathbf{v}_0 = \dot{\mathbf{Z}} = \text{const} \quad (10)$$

where  $\mathbf{E}$  is given by

$$\mathbf{E} = \int_r (\sigma d\tau / 4\pi\epsilon_0)(\xi/\xi^3) \quad (11)$$

The vector  $\xi$  connects the volume element  $d\tau$  to the point at which  $\mathbf{E}$  is to be evaluated. The integral is over all space, but contributions are obtained only from within the sheath, since  $\sigma = 0$  in the plasma.

These two equations indicate that, for fixed vehicle size ( $R_0 = \text{const}$ ), holding  $\sigma/M_+$  constant preserves trajectories. If they are preserved, then  $\sigma_i = K_i\rho_0$ , where  $K_i = \text{const}$ . Since

$$V_s = - \int_r^{r_0} \mathbf{E} \cdot d\mathbf{r}$$

it will not be constant. Table 1 illustrates these relationships.

When the physical size of the vehicle is altered,  $U$  must increase in proportion to  $R_0$ , and the value of  $V_s$  is affected by changes in both factors in its integrand. For example, three equivalent ion flow patterns are as shown in Table 2.

### Summary

Results have been presented of an analytical and an experimental examination of the plasma-vehicle interaction. For that condition in which the vehicle is stationary within the plasma, the fields, potentials, and currents to the vehicle are calculable from Poisson's equation. It was shown that the perturbed region in the plasma may extend outward from the vehicle over distances that are many times greater than the size of the vehicle. It was also noted that the electric field strength on the surface of the vehicle may be greatly enhanced by the sheath.

When the vehicle velocity becomes comparable to, or greater than, the ionic velocity, the simple calculational treatment is no longer valid. Under these conditions, an experimental examination using a vehicle in a plasma stream has been undertaken. The size of the sheath has been examined and its shape found complicated. Ion flow patterns in the downstream region have been examined. For small negative vehicle potentials, a "shadow" was cast by the vehicle in the plasma stream. For increasing negative vehicle potentials, the lens effects of the electric fields from the vehicle have produced ion current peaks in the center of this

**Table 2** Three equivalent cases of a vehicle traveling through a plasma showing the effect of a change in vehicle size

	Case		
	I	II	III
$R_0$ , cm	5	50	50
$U$ , cm/sec	$1 \times 10^6$	$1 \times 10^7$	$1 \times 10^7$
$\rho_0$ , ions/cm <sup>3</sup>	$1 \times 10^6$	$1 \times 10^6$	$1 \times 10^5$
$M_+$ , amu	100	100	10
$V_s$ , v	-100	-10 000	-1000

formerly shadowed region, with an increasing area of diminished ion flow away from these current peaks. These features were predicted by the Davis and Harris<sup>2</sup> calculation. The current flow to the vehicle surface for these negative vehicle potentials has demonstrated the onset of intercepted ions to the backward hemisphere. A final series of measurements has been made of the electric field strength on the vehicle surface. The enhancement of this electric field strength has been measured, and the dependence of this enhancement upon plasma density and position on the vehicle surface has been studied. This enhancement has been demonstrated to be considerably more complex than in the calculable, stationary plasma case.

In addition to providing some details of the plasma vehicle interaction, this work serves to demonstrate the feasibility of the plasma wind tunnel. With the aid of the scaling relationships discussed, many aspects of the interaction of a spacecraft with its environment may be measured in the laboratory.

### References

- Brundin, C. L., "Effects of charged particles on the motion of an earth satellite," *AIAA J.* **1**, 2529-2537 (1963).
- Davis, A. H. and Harris, I., "Interaction of a charged satellite with the ionosphere," *Rarefied Gas Dynamics*, edited by L. Talbot (Academic Press, New York, 1961), pp. 691-699.
- Langmuir, I. and Blodgett, K. B., "Currents limited by space charge between concentric spheres," *Phys. Rev.* **24**, 49-59 (1924).
- Langmuir, I. and Mott-Smith, H. M., "The theory of collectors in gas discharges," *Phys. Rev.* **28**, 727-763 (1926).
- Allen, J. E., Boyd, R. L. F., and Reynolds, P., "The collection of positive ions by a probe immersed in a plasma," *Proc. Phys. Soc. (London)* **B70**, 297-304 (1957).
- Medicus, G., "Theory of electron collection of spherical probes," *J. Appl. Phys.* **32**, 2512-2520 (1961).
- Bernstein, I. B. and Rabinowitz, I. N., "Theory of electrostatic probes in a low-density plasma," *Phys. Fluids* **2**, 112-121 (1959).
- Hall, D. F., Kemp, R. F., and Sellen, J. M., Jr., "Plasma-vehicle interaction in a plasma stream," *AIAA Preprint* 63055 (March 1963).
- Johnson, F. S., *Satellite Environment Handbook* (Stanford University Press, Stanford, Calif., 1961), Chap. 2.
- Sellen, J. M., Jr. and Kemp, R. F., "Cesium ion beam neutralization in vehicular simulation," *IAS-ARS Preprint* 61-84-1778 (June 1961).
- Meckel, B. B., "Experimental study of the interaction of a moving body with a plasma," *Rarefied Gas Dynamics*, edited by L. Talbot (Academic Press, New York, 1961), pp. 701-714.
- Bourdeau, R. E., "Ionospheric results with sounding rockets and the Explorer VIII satellite," *Space Research II*, edited by H. C. Van de Hulst, C. de Jager, and A. F. Moore (North-Holland Publishing Company, Amsterdam, 1961), Part V, pp. 567-568.